List of Illustrations

Figure 1	1st generation optically-controlled optical gate (OCOG) device operation schematic
Figure 2	1st generation OCOG reflectivity gating data and simulation
Figure 3	Demonstration of optically-gated signal gain
Figure 4	2nd generation OCOG device structure
Figure 5	2nd generation OCOG device operation schematic
Figure 6	Effect of number of multiple layers on device speed: data and simulation
Figure 7	2nd generation small-signal response and simulation
Figure 8	2nd generation large-signal response
Figure 9	Demonstration of multiple-pulse operation

MASTER COPY KEEP FOR REPRODUCTION PURPOSES

REPORT DOCUMENTATION PAGE

Form Approved
OMB NO. 0704-0188

1. AGENCY USE ONLY *(Leave blank)*	2. REPORT DATE	3. REPORT TYPE AND DATES COVERED
	July 14, 2000	Final Report

4. TITLE AND SUBTITLE
ULTRAFAST QUANTUM WELL OPTOELECTRONIC DEVICES

5. FUNDING NUMBERS
DAAG55-97-1-0159

6. AUTHOR(S)
David A. B. Miller

7. PERFORMING ORGANIZATION NAMES(S) AND ADDRESS(ES)
Stanford University
Ginzton Laboratory, Mail Code 4085
Stanford, CA 94305-4085

8. PERFORMING ORGANIZATION REPORT NUMBER

9. SPONSORING / MONITORING AGENCY NAME(S) AND ADDRESS(ES)
U.S. Army Research Office
P.O. Box 12211
Research Triangle Park,, NC 27709-2211

10. SPONSORING / MONITORING AGENCY REPORT NUMBER
ARO 37320.1-EL

11. SUPPLEMENTARY NOTES
The views, opinions and/or findings contained in this report are those of the author(s) and should not be construed as an official Department of the Army position, policy or decision, unless so designated by other documentation.

12a. DISTRIBUTION / AVAILABILITY STATEMENT
Approved for public release; distribution unlimited.

12b. DISTRIBUTION CODE

13. ABSTRACT ***(Maximum 200 words)***

This project investigated novel optoelectronic switching and gating devices. These are based on the use of quantum well structures and electronic diodes. The devices can be used as optically controlled optical gates, allowing one light signal to pass in response to the presence of another optical signal, with the gating controlled by applied or induced electrical biases. Though the devices are internally optoelectronic, an important feature is that the speed of operation of the device is governed by very fast internal electrical processes, not by external properties such as the resistive-capacitive time constant of the entire device or the external circuit. Another feature of the device is that the operating optical energies are relatively low. The project has successfully demonstrated several different generations of devices, including a version using one quantum well diode and an advanced structure using two separate diodes. This latter structure allowed higher speed switching because it avoided the necessity for photogenerated carriers to escape from the quantum wells. Device speeds in the picosecond range and burst repetition rates of approximately 50 GHz have been demonstrated. The operation of the device has also been successfully modeled, including a novel multilayer modeling method.

14. SUBJECT TERMS	15. NUMBER IF PAGES
optical gate, optoelectronic, modulator, diffusive conduction, multiple quantum well	16. PRICE CODE

17. SECURITY CLASSIFICATION OR REPORT	18. SECURITY CLASSIFICATION OF THIS PAGE	19. SECURITY CLASSIFICATION OF ABSTRACT	20. LIMITATION OF ABSTRACT
UNCLASSIFIED	UNCLASSIFIED	UNCLASSIFIED	UL

Statement of Problem Studied

There is increasing research interest in making ultrafast switching devices as the bit rates required in long distance and networked telecommunications has risen and as other demanding communications concepts start to be explored, such as very broad band communications (e.g. 1 Tb/s) on the battle field. Ultrafast (e.g., picosecond) optical technology in principle offers ways to make very high speed time-division multiplexing, wavelength-division multiplexing, or switching.

Various ideas for ultrafast switches and physical mechanisms to make them possible have been explored in the past, and many of these are under active study. One of the key difficulties in making conceivably practical devices is that the nonlinear mechanisms, though sensitive enough for laboratory demonstrations, still typically take more optical energy than is desirable for many applications. Another problem is that the effects often do not have the desired speed of response, being sometimes too slow for the application (as is often the case with semiconductor saturable absorption nonlinearities), being faster than desired but with correspondingly weak nonlinear effects (as is the case with glass fiber), or may have undesired slow mechanisms that limit how soon the device may be re-used for a subsequent ultrafast operation. Yet another problem with many high speed optical devices is that they are not readily interfaced to the electronic world.

A new class of optoelectronic devices has been proposed. The devices proposed here could variously permit (i) gated detection of ultrafast optical pulses, allowing conventional electronic circuits to detect the presence of absence of a short optical pulse within a time window; (ii) logic operations between short optical pulses; (iii) signal amplification based on a weak short optical pulse modulating a stronger pulse.

The devices have several interesting practical features. They should offer high sensitivity, as much as 50 times that of devices based on absorption saturation, for example. They should work at room temperature, and based on previous experience with multiple quantum well diodes, can likely be make with high yield, and can be effectively and efficiently integrated, in large numbers, with electronic circuits for read-out and control. The basic devices should operate on a time scale of 10 picoseconds, with higher speeds in the advanced devices. These devices therefore offer seriously interesting practical prospects for ultrafast optical and optoelectronic devices.

Summary of the Most Important Results

Project Title Ultrafast Quantum Well Optoelectronic Devices

Specific Aims Model, design, and test a new class of optoelectronic devices that would be capable of performing (1) gated photodetection of ultrafast optical pulses allowing electronic circuits to detect the presence or absence of a short optical pulse, (2) logic operations between short optical pulses, or (3) signal amplification based on a weak optical pulse modulating a stronger pulse. These devices should be sensitive to low optical powers, operable at room temperature, and integrable in large numbers with electronic circuitry.

Summary Highlights

1st Generation Device:

Demonstration of optically-controlled optical gating
- ~50 ps gate
- 30% absolute reflectivity change, 2:1 contrast ratio
- room temperature operation
- low switching energy, 750fJ (5fJ/μm^2)

Demonstration of signal gain by nearly factor of 2

Development of large-signal simulation model for p-i(MQW)-n diode
- based on diffusive conduction
- hole escape time limits device speed

2nd Generation Device:

Demonstration of optically-controlled optical gating and wavelength conversion
- 11 ps full-width 10% maximum-change, small signal
- 20 ps full-width 10% maximum-change, large signal
  30% absolute reflectivity change, 2:1 contrast ratio
  low switching energy 1.5 pJ (40 fJ/μm^2)
- wavelength conversion: 427 nm signal data transferred to inverted 850 nm signal

Demonstration of multiple-pulse operation at 50GHz burst-logic rate

Development of multilayer diffusive conduction theory
- device recovery speed can be significantly improved using multiple layers

Development of small-signal multilayer simulation

Details – 1st Generation

The first generation device we built was a reverse-biased p-i(100 quantum well)-n GaAs/AlGaAs structure whose reflectivity may be changed by a control pulse of light. Device operation is depicted in Figure 1. The device may be made initially opaque by appropriate biasing. If a control pulse hits the device, its light is absorbed in the QWs. Due to the bias-induced electric field, the photogenerated electrons and holes escape from the QWs and are pulled toward the n and p regions, respectively. As they move, these same charges screen the reverse bias, blue-shifting the exciton absorption peak due to the quantum confined Stark effect (QCSE).[i] While this screening lasts, the effective absorption of the device is reduced, allowing a second, signal pulse to be strongly transmitted (or in the presence of a buried mirror, strongly reflected). The "turn-on" time of the device depends on the escape and subsequent transport of the photogenerated electrons and holes. Using ultrathin (5 angstrom) barriers between the (100 angstrom thick) quantum wells we hoped to both improve modulation speed via tunneling or field-assisted tunneling as well as to increase contrast with a larger number of QWs for a given length of the intrinsic region.

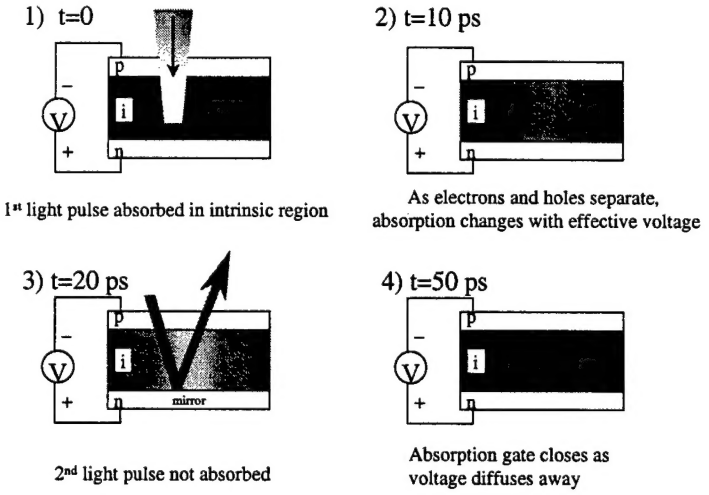

Figure 1. Schematic of the p-i(MQW)-n diode (1st generation) optically controlled optical gate device operation with picosecond pulses

As mentioned above, the duration of the strongly reflecting state (the "ON" state of the device) will last only while the bias voltage remains screened. The decay mechanism of this screening is due to diffusive conduction.[ii] Since this decay mechanism does not require the initial photo-generated charge to be removed, speed is not limited by external RC time constants or carrier lifetimes. If the spot size of the control pulse is small with respect to the surface area of the device, then as the photocarriers vertically separate, they will build up a localized screening voltage which views the device as a 2D dissipative wire: there is a capacitance per unit area across the intrinsic region (vertically), while there is a resistance per square across the p and n regions (horizontally). As such, the voltage obeys a diffusion equation given by

$$\frac{dV}{dt} = D\nabla_{xy}^2 V \qquad (1)$$

where the diffusion coefficient is simply $D=1/R_{SQ}C_A$; here R_{SQ} is the sum of the resistances per square of the p and n regions and C_A is the capacitance per area across the intrinsic region. Because it is the voltage and not the carriers themselves which dissipates and spreads, this effect is not limited by carrier diffusion, and because the device can effectively recover through local diffusive conduction the recovery time is not dominated by the external circuitry (and its relatively long RC time constants). More accurately, there are two different time constants of interest: (i) the optical modulation recovery time and (ii) the overall electronic recovery time, which does depend on carrier relaxation through external circuitry.

The results are shown in Figure 2. Using a 750fJ pump pulse with a spot size of 7μm radius (~5fJ/μm^2) tuned to 855nm and the device biased at -6.3V, the heavy hole exciton is strongly absorbing. As can be easily seen in the figure, the probe pulse experiences a reflectivity change with a contrast ratio of

1.8-to-1 and an absolute change in reflectivity of 0.3. The high-reflectivity state of the device induced by the pump pulse decays within about 50ps. The energy needed for switching is very low – less than a picojoule – and compares very favorably with the other switching mechanisms.

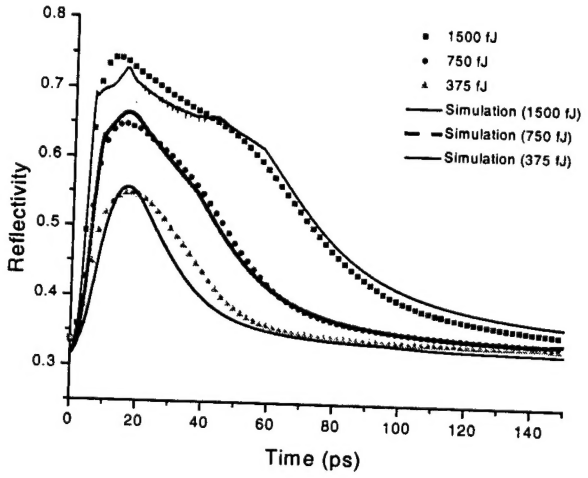

Figure 2. Reflectivity modulation of probe (signal) pulse as a function of time with -6.3V bias across device and 855nm light at various pump (control) pulse powers with a spot size of 50um^2. Simulation [solid lines] reflectivity modulation at various input powers. The good fit of the tails to a hyperbolic decay is a good indication that diffusive conduction is responsible for the voltage dissipation.

Figure 2 also compares medium and large-signal data to simulation. The simulation model includes the following parameters: a gaussian distribution for the creation of electrons and holes based on the spot size of the pulse; effective escape times from the wells for both electrons and holes; vertical field-dependent velocity – also for both carrier types; a diffusion coefficient and voltage decay mechanism derived from Eq. 1; and measured results relating bias voltage to absorption. The close fit between data, particularly for the tails, gives strong support for our hypothesis that it is indeed diffusive conduction that is the mechanism primarily responsible for voltage decay.

The device recovery time is long, especially when compared to the expected rapid voltage diffusion time coefficient that is on the order of a picosecond. We believe this may be due to a long hole escape time from the quantum wells. Reducing the hole escape time should make this type of device significantly faster.

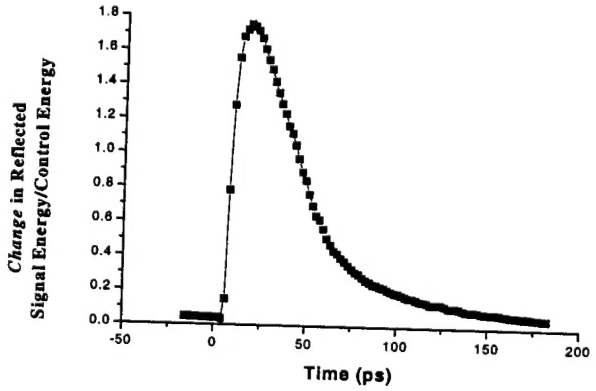

Figure 3. Signal gain vs. time -- more specifically, change in reflected probe (signal) power normalized against pump (control) pulse power – with the device biased at -6.0V, pump power of 750fJ and probe power of 2.56pJ at 855nm.

The percentage change in probe reflectivity – induced by the pump pulse -- should be nominally independent of probe power. Normally the pump pulse induces changes in reflected probe power which are small compared to the pump power. However, if the incoming probe power is made large compared to the pump, the changes in reflected probe power can be larger than the pump power itself – in effect creating gain in the reflected signal. Fig. 3 demonstrates this, showing gain close to a factor of 2.

In summary, we demonstrated an optically controlled surface-normal switch that can be switched in 50ps with reflectivity swings from 0.3 to 0.6. This type of device should be integrable with CMOS (via flip-chip bonding), acting concurrently as a photodetector at CMOS speeds by measuring the photo-induced current as well as allowing control of the switch operation through the bias voltage. The quantum confined Stark effect and diffusive conduction are the mechanisms primarily responsible for the large change in reflectivity and fast recovery time, respectively. Signal gain using the same device was also shown.

Details – 2nd Generation

The second generation device is an optically controlled optical gate composed of two p-i-n diodes on top of a distributed Bragg reflector (DBR) mirror, as shown in Figure 4. The bottom (modulator) diode, which embodies multiple quantum wells (MQW) in its intrinsic region, has its absorption switched when an incident control pulse is absorbed in the top (control) diode.

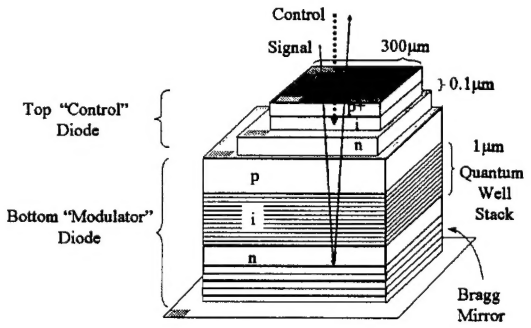

Figure 4. Device schematic of a double diode structure with an ITO deposition over a thin top diode (100 nm intrinsic region) and a p-i(MQW)-n bottom diode.

The control diode, operated under reverse bias, is designed to be transparent to the signal (probe) pulse, but opaque to the control (pump) pulse, which is at a shorter wavelength. The modulator diode is initially reverse-biased so that the quantum wells are substantially transparent to the signal; the system is in its highly reflective state for the signal. When the control pulse hits the top diode, it is fully absorbed, creating electrons and holes primarily in the control diode's bulk intrinsic region. Because of the reverse bias, these photogenerated electrons and holes migrate to the n-region and p-regions, respectively. Unlike the first generation device, there are no quantum wells in the top diode so esacape time is not a concern. As the carriers vertically separate, they locally screen the bias-induced electric field, decreasing the reverse voltage across the top diode in the vicinity of the control pulse spot. As a consequence of the dual-diode structure (see below), the reverse bias voltage on the bottom diode is locally *increased*, thereby making the quantum wells more absorbing through quantum confined Stark effect (QCSE), and reducing the reflectivity of the signal. The voltage build-up time, and hence the "turn-on" time of the device, is determined by the transport times of carriers in the bulk material, ~1ps for the thin intrinsic region of the top diode. The "turn-off" time of the device is controlled by the local electrical relaxation of the voltage across the diodes through diffusive conduction. A schematic of the second generation's optical gate operation is presented in Figure 5.

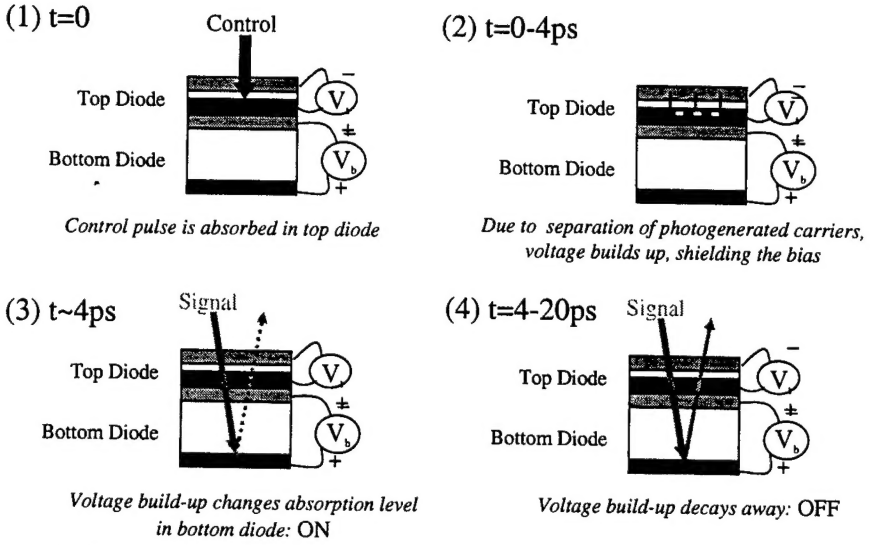

Figure 5. Schematic of the dual diode (2nd generation) optically controlled optical gate device operation with picosecond pulses

This dual diode structure can be modeled as three multiple dielectric layers (2 intrinsic regions and the depletion region between the middle p and n regions), each sandwiched between conducting layers (p- and n-regions). The highly conducting top-most and bottom-most layers of the entire device force the structure to keep the voltage across it effectively constant. Therefore, any local voltage *reduction* in the top diode leads to a corresponding local voltage *increase* in the bottom diode. The voltage behavior across a single layer, however, is dependent on the other layers in the device and is coupled to the other voltages. A theory has been developed which accounts for this coupling and provides a method to calculate the voltage dynamics for an arbitrary number of layers.[iii]

The system dynamics may be described by

$$\frac{\partial}{\partial t}\tilde{V} = \tilde{\tilde{D}}\tilde{\mathrm{N}}^2\tilde{V} \tag{2}$$

where $\tilde{V}$ is the vector of the voltages across the intrinsic layers and $\tilde{\tilde{D}}$ is the diffusion coupling matrix between the layers. To solve this system of equations, the general approach taken is composed of four steps: (1) determine the coupling diffusion matrix, $\tilde{\tilde{D}}$; (2) solve the eigenvector problem to describe a decoupled system; (3) apply the solution to the regular (uncoupled) diffusion equation for the eigenvectors; (4) transform the dynamic solution back to the original variables. Steps (2)-(4) are relatively straightforward. All that is needed is to determine the original coupling matrix, $\tilde{\tilde{D}}$, which be determined from the following relationship

$$\tilde{\tilde{D}} = \frac{1}{\tilde{C}}\tilde{\tilde{M}}^{-1}_{1[N]}\frac{1}{\tilde{R}_{[N]}}\tilde{\tilde{M}}^{-1}_{2[N]} \tag{3}$$

The division of $\tilde{R}$ (a vector related to the resistance per square of each resistive plane) and $\tilde{C}$ (the capacitance per unit area of each layer) mean element-by-element operations instead of matrix operations, and $\tilde{\tilde{M}}^{-1}_{1[N]}$ and $\tilde{\tilde{M}}^{-1}_{2[N]}$ are determined simply by the number of layers.[iii]

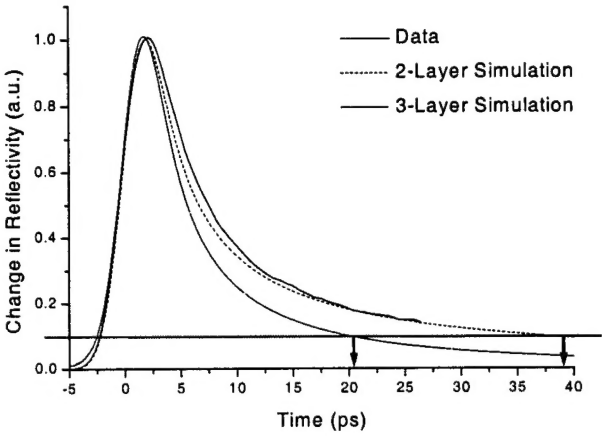

Figure 6. Small signal response of the OCOG with an effective 2-layer structure compared to simulations of both 2 and 3-layer structures. Note the significant improvement in gate speed closure (blue arrows indicate a return to with 10% of initial conditions) in the presence of an additional layer.

Having the ability to accurately model the voltage behavior across multi-layer resistive and capacitive stacks is essential for understanding a stacked diode OCOG. As seen in Figure 6, the presence of extra layers is shown to have a profound impact on the recovery time of the device. This same analysis method may also be used to help study n-i-p-i devices. Multilayer diffusive conduction analysis has also helped to reveal a useful insight. In analogy with the frequency response of an electrical RC circuit in which the presence of extra RC filters changes the system's filter response (e.g. adding an extra 6dB/octave per set, modified by the extra load), the presence of extra layers significantly speeds up the voltage decay response, although at a cost of reduced voltage swing. This is particularly relevant for diffusive conduction behavior since its hyperbolic decay, although fast at small times, slows down considerably at times large with respect to the diffusion coefficient time constant. The presence of multiple layers provides a method which enables the voltage to drop even more rapidly at the beginning so that by the time the fall-off diminishes, it is significantly lower than it might otherwise have been. The result is not a faster effective diffusion time constant; rather, the response function itself is changed, more closely resembling the multiplication of the individual diffusive conduction decays. As Figure 6 shows, adding additional layers results in significantly reduced decay times necessary to recover to, say, 10% of the peak voltage. The data in Figure 6 was obtained by shorting the middle p- and n-regions together to remove the effects of the depletion region, creating a 2-layer device.

Small-signal behavior of this device, with a 70 fJ switching energy, showing an 11.3 ps turn on-off time is presented in Figure 7. Using expected or measured values for pulse width (2 ps), spot size (3.5 μm radius), layer thicknesses and resistivity, as Figure 7 demonstrates, there was very close agreement between theory (three-layer model) and recorded data.

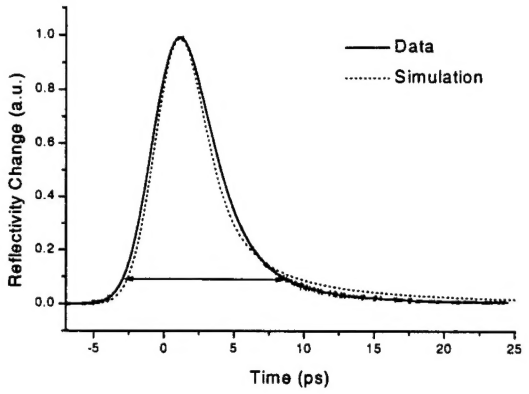

Figure 7. Small signal response of the optical gate, with a 11.3 ps full-width 10% maximum (indicated by the horizonal, arrowed line) turn on-off time.

Large-signal device behavior (not simulated) is presented in Figure 8. The spot size radius was again 3.5 μm, while the switching energy was 1.5 pJ (39 fJ/μm^2). Excluding the parasitic absorption of the ITO (described above) and top p-layer, approximately a 2-to-1contrast ratio was achieved with a change in absolute reflectivity of about 30%. The optical gate opens and closes -- returns to 10% of maximum change -- within 19.6 ps.

This slightly slower response compared to small signal behavior likely occurs because the carriers fully screen the reverse bias across the top diode before they reach the doped layers, slowing vertical carrier transport.

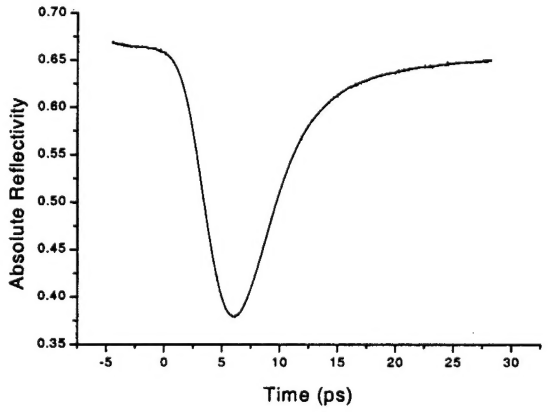

Figure 8. Large-signal response of the optical gate with a 30% reflectivity change.

Figure 9 shows the device's response to four control pulses, each separated by 20 ps. Simulation results match well, with the discrepancy likely due to imperfect matching of the pulse energies in the pulse stream generator. The device's ability to recover in a short time is clearly evident. There is a slight increase in the base reflectivity level for the later pulses due to the build-up of previous pulses' decay. Simulations show that this build-up of base reflectivity (critical if the device is to be used as a modulator at these rates) levels off to a manageable level not far from what is already seen here.

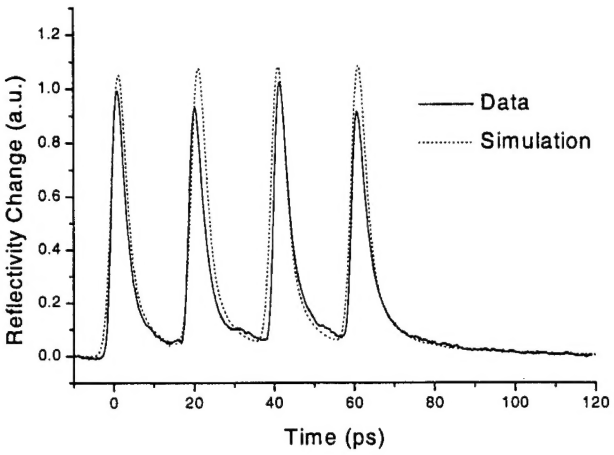

Figure 9. Multiple-pulse, small-signal response of the optical gate with 20 ps pulse separation.

We have demonstrated that a surface normal, optically controlled optical gate turns on and off within 20 picoseconds with a 30% reflectivity change, and that the device can operate with a 20 picosecond pulse repetition period. A small-signal model of voltage behavior across multi-layered structures has been developed and matches the data well, including the intriguing behavior of faster device recovery as the number of layers increases. Future work may include improving processing techniques, optimizing the modulator structure for larger contrast ratios and faster responses, and fully integrating such structures with a CMOS system via flip-chip bonding.

List of Participating Scientific Personnel

Micah B. Yairi - earned Masters Degree in Applied Physics while employed on the project

Hilmi Volkan Demir

Prof. David A.B. Miller

List of Publications and Technical Reports

M. B. Yairi, C. W. Coldren, D. A. B. Miller, and J. S. Harris, "High-Speed Quantum Well Optoelectronic Gate Based on Diffuse Conduction Recovery," in Optics in Computing '98, Pierre Chavel, David A. B. Miller, Hugo Thienpont, Editors, (Optics in Computing '98 Conference, Brugge, Belgium (June 17-20, 1998)) Proc. SPIE Vol. 3490, 10-13 (1998).

M. B. Yairi, C. W. Coldren, D. A. B. Miller, and J. S. Harris, Jr., "High-Speed, Optically-Controlled Surface-Normal Modulator Based on Diffusive Conduction," Appl. Phys. Lett., 75 (5), 597-599 (1999).

M. B. Yairi, H. V. Demir, C. W. Coldren, D. A. B. Miller, and J. S. Harris, "Optically-Controlled Optical Gate Using a Double Diode Structure," in IEEE Lasers and Electro-Optics Society 1999 Annual Meeting, San Francisco, CA (November 8-11, 1999). Paper ThN2.

M.B. Yairi, H.V. Demir, C.W. Coldren, J.S. Harris, Jr. and D.A.B. Miller, "Demonstration of an optoelectronic dual-diode optically controlled optical gate with a 20-ps repetition period," in Nonlinear Optics: Materials, Fundamentals and Applications, Kauai, HI (Aug 7-10, 2000). Paper MB2.

M.B. Yairi, H.V. Demir, and D.A.B. Miller, "Optically controlled optical gate with an optoelectronic dual diode structure – theory and experiment," Opt. Quantum Electron. (submitted).

Bibliography

[i] D.A.B. Miller, D.S. Chemla, T.C. Damen, A.C. Gossard, W. Wiegmann, T.H. Wood, and C.A. Burrus, Phys. Rev. **B34**, 1043 (1985).

[ii] G. Livescu, D.A.B. Miller, T. Sizer, D.J. Burrows, J. Cunningham, A.C. Gossard, and J.H. English, Appl. Phys. Lett., **54**, 748 (1989).

[iii] M.B. Yairi, H.V. Demir, and D.A.B. Miller, Opt. Quantum Electron. (submitted)